Bandwidth and Power Efficient Constant-Envelope BPSK Signals

Hyung Chul Park* *Regular Member*

ABSTRACT

The power and bandwidth efficient constant-envelope BPSK (CE-BPSK) modulation is proposed. The CE-BPSK signal is realized specifying the phase transition characteristics for the conventional low pass filtered BPSK signal. Since the CE-BPSK signal has constant envelope and modified waveform, the CE-BPSK signal has better power and bandwidth efficiency compared to the conventional BPSK signal while the CE-BPSK signal is backward compatible to the conventional BPSK signal. It is also shown that the bit error rate performance of the CE-BPSK signal is the same as that of the conventional BPSK signal.

Key words: CE-BPSK, Non-linear amplification, Phase transition, MLSD, symbol-by-symbol detection.

I. Introduction

Because of the simple transmitter and receiver architecture, the binary phase shift keying (BPSK) is still widely used in wireless communication. Recently in 2003, BPSK has been chosen as a modulation for IEEE 802.15.4 wireless personal area network (WPAN) [1]. However, the envelope of the BPSK signal is not constant, causing spectrum regrowth after passing through the non-linear power amplifier. Furthermore, the large back-off for the linear operation of high power amplifier increases the power consumption of the BPSK modulation. If a BPSK signal has constant envelope and compact spectrum as well as can use conventional symbol-by-symbol coherent detection in the receiver, the BPSK becomes both power and band efficient modulation with backward compatibility to the conventional BPSK.

In this paper, a constant envelope BPSK (CE-BPSK) modulation is proposed. The CE-BPSK signal is realized specifying the phase transition characteristics for the conventional low pass filtered BPSK signal. Since the CE-BPSK signal has constant envelope, a non-linear power amplifier, such as a class-C amplifier, can be used without much spectrum regrowth, leading to higher power efficiency. The proposed CE-BPSK signal also has better bandwidth efficiency compared to the conventional BPSK signal in both linear and non-linear amplification environments.

In next section, the both power and bandwidth efficient CE-BPSK modulation is proposed. In Section III, the minimum normalized squared Euclidean distance (MNSED) of the CE-BPSK signal is analyzed. And, the optimum coherent detection for the CE-BPSK signal is derived. In Section IV, the power spectral density (PSD), eye-diagram, and BER performance of the CE-BPSK signal are evaluated and compared with those of the conventional BPSK signals. Finally, Section V presents the conclusion.

II. CE-BPSK Modulation

The conventional BPSK signal is written as

*SoC team, Hynix Semiconductor Inc., Kang-nam, Seoul. (chori@dimple.kaist.ac.kr)
논문번호: 040139-0331, 접수일자: 2004년 4월 1일

$$s(t)=\left(\sum_k A_k \cdot h(t-kT_b)\right)\cdot \cos\omega_c t \qquad (1)$$

where $A_k \in \{-1,+1\}$ is the information data. $h(t)$ denotes the impulse response of the pulse shape function. For the inter-symbol interference free communication, the root-raised cosine filter is widely used as the pulse shape function. In (1), the information data is carried by the carrier phase of 0 or π, which is shown in Fig. 1 (a). Dotted line in Fig. 2 shows the phase transition of the conventional BPSK signal, in which the information data is equal to (-1, 1, 1, 1, -1, -1, 1, -1, -1, 1, 1, -1). However, since the power of the conventional BPSK signal changes between 0 and non-zero value, the power amplifier requires the large back-off. It means that the conventional BPSK modulation is not power-efficient.

Now, lets change the carrier phase mapping as follows. When the information data is equal to +1, the carrier phase is mapped to either $+\pi/4$ or $-\pi/4$ rather than 0. When the information data is equal to -1, the carrier phase is mapped to either $+3\pi/4$ or $-3\pi/4$ rather than π. And, the transient phase moves along the unit circle in the signal constellation. It is shown in Fig. 1 (b).

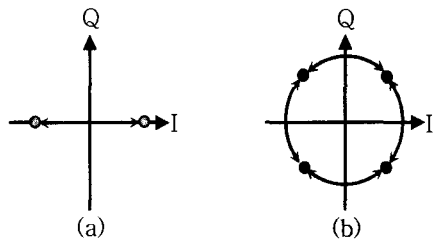

Fig. 1. Signal constellation diagram of (a) conventional BPSK and (b) CE-BPSK signals.

This modified phase transition is shown as solid line in Fig. 2. We can find that at $t=kT_b,(k=0,1,2,\cdots)$, the cosine of the modified phase has the same sign as the conventional BPSK signal.

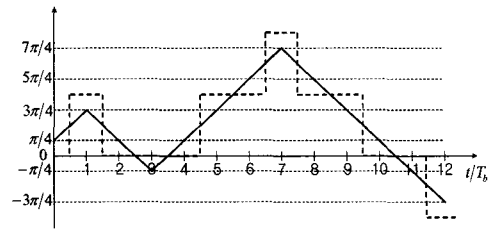

Fig. 2. Phase transition behavior of the BPSK and CE-BPSK signals. Note that the information data is equal to (-1, 1, 1, 1, -1, -1, 1, -1, -1, 1, 1, -1).

Compared with the conventional BPSK signal, the modulated signal based on the modified phase mapping rule has the following characteristics :

1. The modified signal has constant envelope. It makes possible to operate the power amplifier in non-linear saturation region. It means that the modified signal is more power efficient than the conventional BPSK signal.
2. The modified signal has backward compatibility to the conventional BPSK signal. When the information data is equal to +1, the carrier phase for the conventional BPSK signal is equal to 0 and the carrier phase for the modified signal is equal to either $+\pi/4$ or $-\pi/4$. The cosine of the both signal is greater than 0. And, when the information data is equal to -1, the carrier phase for the conventional BPSK signal is equal to π and the carrier phase for the modified signal is equal to either $+3\pi/4$ or $-3\pi/4$. The cosine of the both signal is less than 0.

We propose the CE-BPSK modulation with aforementioned characteristics. The phase transition rule for the CE-BPSK signal is presented in Table 1. In Table 1, a_{n-1} denotes the information data at $t=(n-1)T_b$ and ϕ_n denotes the carrier phase at $t=nT_b$. It is shown that ϕ_{n+1} is determined by a_n and ϕ_n. When a_n is equal

to -1, the cosine of carrier phase at $t=(n+1)T_b$ must be less than 0. Therefore, the carrier phase ϕ_{n+1} must be either $+3\pi/4$ or $-3\pi/4$. When a_n is equal to +1, the cosine of carrier phase must be greater than 0. Therefore, ϕ_{n+1} must be either $+\pi/4$ or $-\pi/4$. The selection between $+3\pi/4(+\pi/4)$ and $-3\pi/4(-\pi/4)$ is determined by ϕ_n in order to limit the phase transition during T_b to $\pi/2$.

Furthermore, if the CE-BPSK signal is differentiable, even at $t=1T_b, 3T_b,$ and $7T_b$ in Fig. 2 that the derivatives of the signals phase change to the opposite sign, better bandwidth efficiency can be achieved. Note that for the every CE-BPSK signals phase to be differentiable, the transient phase between times $t=nT_b$ and $(n+1)T_b$ must depend on ϕ_{n-1} and ϕ_{n+2}. From Table 1, we can find that, when a_n is identical to a_{n-2}, ϕ_{n+1} becomes identical to ϕ_{n-1}. It means that the sign of $\Delta\phi_n$, i.e., $\phi_n-\phi_{n-1}$, is opposite to that of $\Delta\phi_{n+1}$. It implies that the derivative of the signals phase must be equal to 0 at $t=nT_b$. When a_n is different than a_{n-2}, $|\phi_{n+1}-\phi_{n-1}|$ is equal to π. It means that the sign of $\Delta\phi_n$ is equal to that of $\Delta\phi_{n+1}$. It implies that the derivative of the signals phase must be $\pi/(2\sqrt{2}T_b)$ at $t=nT_b$. Note that the aforementioned characteristics are the same at $t=(n+1)T_b$. Consequently, the transient phase between times $t=nT_b$ and $t=(n+1/2)T_b$ is related to a_{n-2} and a_n. And, the transient phase between times $t=(n+1/2)T_b$ and $t=(n+1)T_b$ is related to a_{n-1} and a_{n+1}. In order to satisfy aforementioned characteristics, a waveform pair is proposed. It is written as

$$
\begin{aligned}
f_1 &= \left\{ \begin{bmatrix} 1-(1/3)\cdot(1-1/\sqrt{2})\cdot\cos^2((\pi/2)\cdot(t-nT_b)/(T_b/2)) \\ -(2/3)\cdot(1-1/\sqrt{2})\cdot\cos^4((\pi/2)\cdot(t-nT_b)/(T_b/2)) \\ +\sin(\pi/4+(\pi/4)\cdot(t-nT_b)/(T_b/2))\cdot(a_{n-2}\,\hat{}\,a_n) \end{bmatrix}\cdot\overline{(a_{n-2}\,\hat{}\,a_n)} \right\}\cdot(1-u(t-(n+1/2)T_b)) \\
&+\left\{ \begin{bmatrix} 1-(1/3)\cdot(1-1/\sqrt{2})\cdot\sin^2((\pi/2)\cdot(t-(n+1/2)T_b)/(T_b/2)) \\ -(2/3)\cdot(1-1/\sqrt{2})\cdot\sin^4((\pi/2)\cdot(t-(n+1/2)T_b)/(T_b/2)) \\ +\cos((\pi/4)\cdot(t-(n+1/2)T_b)/(T_b/2))\cdot(a_{n-1}\,\hat{}\,a_{n+1}) \end{bmatrix}\cdot\overline{(a_{n-1}\,\hat{}\,a_{n+1})} \right\}\cdot u(t-(n+1/2)T_b),\ nT_b<t<(n+1)T_b \\
f_2 &= \left\{ \begin{bmatrix} -(1/2)\cdot\cos((\pi/2)\cdot(t-nT_b)/(T_b/2)) \\ +(1/2-1/\sqrt{2})\cdot\cos^3((\pi/2)\cdot(t-nT_b)/(T_b/2)) \\ -\cos(\pi/4+(\pi/4)\cdot(t-nT_b)/(T_b/2))\cdot(a_{n-2}\,\hat{}\,a_n) \end{bmatrix}\cdot\overline{(a_{n-2}\,\hat{}\,a_n)} \right\}\cdot(1-u(t-(n+1/2)T_b)) \\
&+\left\{ \begin{bmatrix} (1/2)\cdot\sin((\pi/2)\cdot(t-(n+1/2)T_b)/(T_b/2)) \\ -(1/2-1/\sqrt{2})\cdot\sin^3((\pi/2)\cdot(t-(n+1/2)T_b)/(T_b/2)) \\ +\sin((\pi/4)\cdot(t-(n+1/2)T_b)/(T_b/2))\cdot(a_{n-1}\,\hat{}\,a_{n+1}) \end{bmatrix}\cdot\overline{(a_{n-1}\,\hat{}\,a_{n+1})} \right\}\cdot u(t-(n+1/2)T_b),\quad nT_b<t<(n+1)T_b
\end{aligned}
\tag{2}
$$

where $\hat{}$ denotes XOR operator. a_n is equal to {0,1} rather than {-1,+1} for the convenience of presentation. The unit step function $u(t)$ is defined as

$$
u(t)=\begin{cases} 0, & t<0 \\ 1, & t>0 \end{cases} \tag{3}
$$

The waveforms for I and Q channel signal of CE-BPSK modulation are presented in Table 1.

Table 1. Phase transition rule for the CE-BPSK signal and corresponding I and Q channel signal.

a_{n-1}	ϕ_n	a_n	ϕ_{n+1}	I ch. signal	Q ch. signal
+1	$-\pi/4$	-1	$-3\pi/4$	(-1)* f_2	(-1)* f_1
		+1	$+\pi/4$	f_1	f_2
	$+\pi/4$	-1	$+3\pi/4$	(-1)* f_2	f_1
		+1	$-\pi/4$	f_1	(-1)* f_2
-1	$-3\pi/4$	-1	$+3\pi/4$	(-1)* f_1	f_2
		+1	$-\pi/4$	f_2	(-1)* f_1
	$+3\pi/4$	-1	$-3\pi/4$	(-1)* f_1	(-1)* f_2
		+1	$+\pi/4$	f_2	f_1

III. Optimum Coherent Detection of the CE-BPSK Signals

The bit error probability is an important figure of merit for a digital modulation [2]. In [3], it was noted that the probability of error $P(e)$ is bounded by the union bound. It is written as

$$P(e)=\frac{1}{N}\sum_{i=0}^{N-1}P(e|m_i)\le\frac{1}{N}\sum_{i=0}^{N-1}\sum_{\substack{j=0\\(j\neq i)}}^{N-1}Q\left(\sqrt{d_{ij}^2\frac{E_b}{N_0}}\right) \quad (4)$$

where N is the total number of signal alternatives, $m_0, m_1, \cdots, m_{N-1}$ and $Q(x)$ is defined as

$$Q(x)=\frac{1}{\sqrt{2\pi}}\int_x^\infty e^{-t^2/2}dt \quad (5)$$

d_{ij}^2 denotes the squared Euclidean distance (ED) in signal space between m_i and m_j, normalized by $2E_b$, which is written as [4]

$$d_{ij}^2=\frac{1}{2E_b}\int_0^\infty (m_i-m_j)^2dt \quad (6)$$

When E_b/N_0 is large, the union bound becomes tight and dominated by the MNSED $d_{\min}^2$. It is written as

$$P(e)\approx C\cdot Q\left(\sqrt{d_{\min}^2\frac{E_b}{N_0}}\right) \quad (7)$$

where error coefficient C is equal to 1 for CE-BPSK signal.

In order to calculate the MNSED of the CE-BPSK signal, it is necessary to examine the phase behavior of the CE-BPSK signal. Note that the CE-BPSK signal is a kind of PSK since the information is carried by the absolute phase. So, the Euclidean distance between two CE-BPSK signals, in which there is only 1 bit different between two information data sequence, becomes MNSED. These two information sequences are written as

$$\mathbf{a}_0=\{\cdots,a_{n-1},-1,a_{n+1},\cdots\}$$
$$\mathbf{a}_1=\{\cdots,a_{n-1},1,a_{n+1},\cdots\} \quad (8)$$

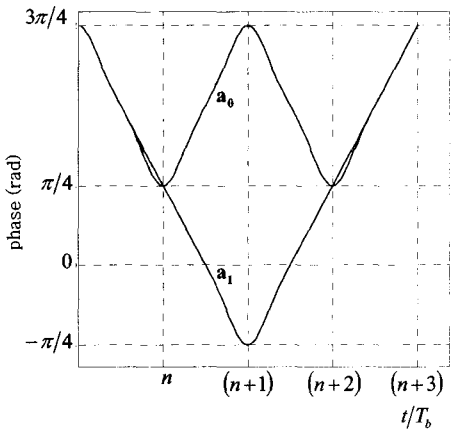

Fig. 3. Transient phase pair for the MNSED calculation.

For example, lets assume that ϕ_n is equal to $+\pi/4$, $\mathbf{a}_0$ and $\mathbf{a}_1$ between times $t=(n-1)T_b$ and $(n+2)T_b$ are {+1,-1,+1,-1} and {+1,+1,+1,-1}, respectively. Corresponding transient phases are shown in Fig. 3.

At $t=(n+1)T_b$, the carrier phase for the CE-BPSK signal with $\mathbf{a}_0$ becomes equal to $+3\pi/4$. And, the carrier phase with $\mathbf{a}_1$ becomes equal to $-\pi/4$. At $t=(n+2)T_b$, the carrier phase with $\mathbf{a}_0$ and $\mathbf{a}_1$ become both equal to $+\pi/4$. Fig. 3 shows that the phase merge between two CE-BPSK signals has length $3T_b$. Therefore, MNSED of the CE-BPSK signal $d^2_{\min}$ is written as

$$d^2_{\min}=\frac{1}{2E_b}\int_{(n-1/2)T_b}^{(n+5/2)T_b}\left(s(t,\phi_n,\mathbf{a}_0)-s(t,\phi_n,\mathbf{a}_1)\right)^2 dt \quad (9)$$

The calculated MNSED of the CE-BPSK signal is equal to 2.

In Section II, it has been shown that the selection between two phase points which have same cosine, i.e., $\{+3\pi/4,-3\pi/4\}$, $\{+\pi/4,-\pi/4\}$, depends on the phase at the previous symbol time. It means that the coherent detection utilizing the phase transition trajectory can achieve better BER performance than the symbol-by-symbol coherent detection. This is maximum likelihood sequence detection (MLSD), in which a state is the carrier phase at every symbol time, i.e., $-\pi/4,+\pi/4,+3\pi/4$, and $-3\pi/4$. Fig. 4 shows the state and state transition on the coherent MLSD for the CE-BPSK signal.

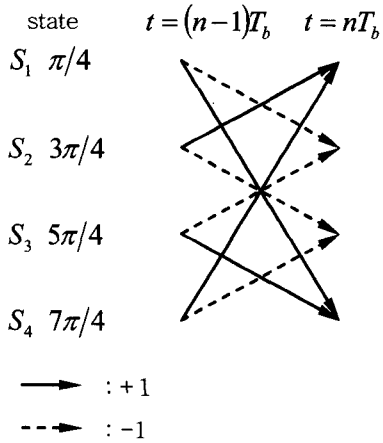

Fig. 4. State and state transition on the coherent MLSD for the CE-BPSK signals.

The branch metric for the MLSD between times $t=(n-1)T_b$ and $t=nT_b$ is the Euclidean distance between the received signal $r(t)$ and the allowed signal $s(t,\phi_{n-1},a_{n-1})$, which is presented in Table 1. It is written as

$$d^2_{branch\,metric}=\int_{(n-1)T_b}^{nT_b}\left[r(t)-s(t,\phi_{n-1},a_{n-1})\right]^2 dt \quad (10)$$

During the trace-back process, when the state is equal to $+\pi/4$ or $-\pi/4$, the receiver decides that a +1 was sent. Otherwise, it decides that a -1 was sent.

IV. Performance Evaluation

Fig. 5 shows the PSD of the proposed CE-BPSK signal in linear amplification environment. It shows that the bandwidth efficiency of the CE-

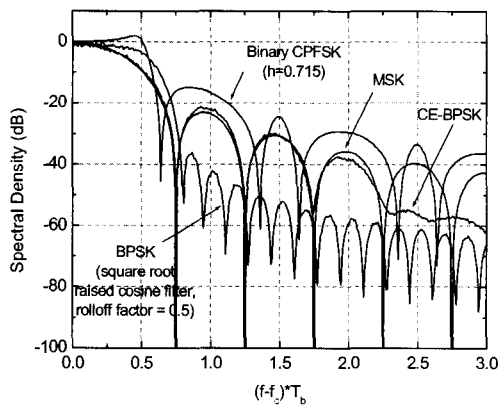

Fig. 5. PSD of the CE-BPSK signal in linear amplification environment.

BPSK signal is almost the same as that of the conventional BPSK and MSK signal. It is presented in Table 2. The root-raised cosine filter with a roll-off factor of 0.5 is used for the conventional BPSK signal. Furthermore, it is better than the bandwidth efficiency of the optimum binary CPFSK signal.

Fig. 6 shows the PSD of the CE-BPSK signal in non-linear amplification environment. Note that since the CE-BPSK signal has constant envelope, the PSD is not changed in non-linear amplification environment while the conventional BPSK signal suffers severe PSD regrowth.

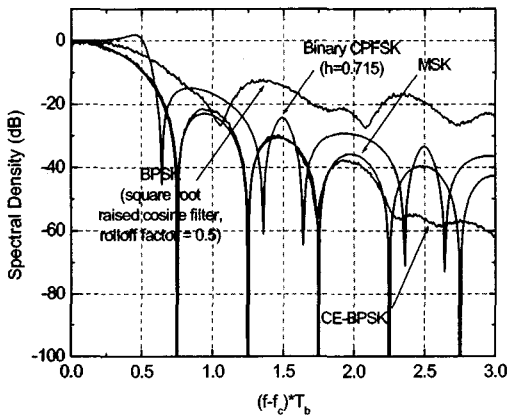

Fig. 6. PSD of the CE-BPSK signals in non-linear amplification environment.

In Table 2, the bandwidth efficiency of the CE-BPSK signal is compared quantitatively with that of the conventional BPSK, MSK, and optimum binary CPFSK signal with a modulation index of 0.715 in linear and non-linear amplification environments. The bandwidth is defined as the ratio of the frequency band around the carrier frequency containing 99% of the signal power to the data rate.

Table 2. Bandwidth efficiency of the CE-BPSK signal in linear and non-linear amplification environments.

	Linear amplification Hz/(b/s) (two-sided)	Non-Linear amplification Hz/(b/s) (two-sided)
CE-BPSK	1.25	1.25
Binary CPFSK (h=0.715)	1.81	1.81
MSK	1.19	1.19
BPSK	1.27	15.8

Fig. 7 shows the eye diagram of the CE-BPSK signals.

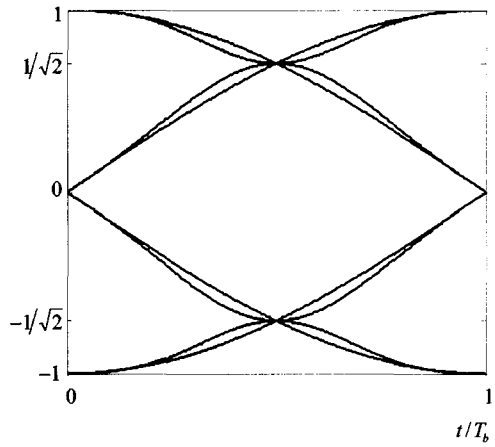

Fig. 7. Eye diagram of the CE-BPSK signals.

Fig. 8 shows the simulated BER performance of the linearly amplified CE-BPSK signal with MLSD in AWGN channel. It shows that the BER of the CE-BPSK signal is the same as that of the linearly amplified conventional BPSK signal.

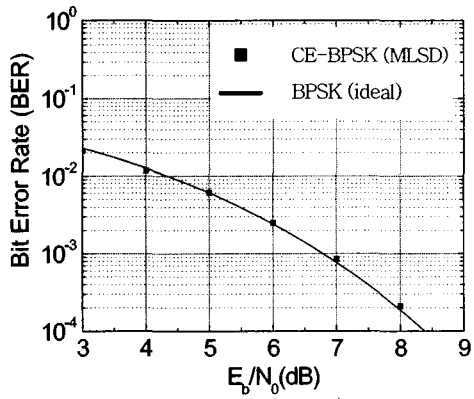

Fig. 8. BER performance of the CE-BPSK modulation with MLSD.

V. Conclusions

In this paper, the CE-BPSK modulation has been proposed. Proposed waveform and phase transition rule make it possible for the CE-BPSK signal to have better power and bandwidth efficiency compared to the conventional BPSK signal.

Since the bandwidth efficiency of the CE-BPSK signal is almost the same as that of the conventional BPSK signal, the RF transmitter (except the power amplifier) and receiver for the conventional BPSK signal can be used without modification.

Simulation result has shown that the bit error rate performance of the CE-BPSK signal is the same as that of the conventional BPSK signal.

Acknowledgement

The author would like to thank Prof. Kwyro Lee of Korea Advanced Institute of Science and Technology (KAIST) for the helpful discussion and encouragement.

References

[1] Institute of Electrical and Electronics Engineers, Inc., IEEE Std. 802.15.4-2003, Wireless Medium Access Control (MAC) and Physical Layer (PHY) Specifications for Low Rate Wireless Personal Area Networks (WPAN). New York: IEEE Press. 2003.

[2] B. Sklar, Digital Communications, Englewood Cliffs, N. J.: Prentice Hall, 1988.

[3] J. M. Wozencraft and I. M. Jacobs, Principles of Communication Engineering. New York: Wiley, 1965, pp. 264-266.

[4] T. Aulin and C. E. Sundberg, Continuous Phase Modulation-Part I: Full Response Signaling, IEEE Trans. Commun., vol. COM-29, no. 3, pp. 196-209, Mar. 1981.

Hyung Chul Park

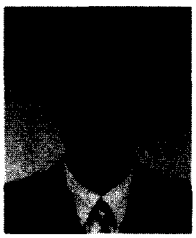

Feb. 1996: B.S. degree in electrical engineering from Korea Advanced Institute of Science and Technology (KAIST).

Feb. 1998: M.S. degree in electrical enginee- ring from KAIST.

Feb. 2003: Ph.D. degree in electrical enginee- ring and computer science from KAIST.

Feb. 2003 ~ : Hynix Semiconductor Inc. He is a Manager in SoC team.

Research interests: wireless modulation/ demodulation algorithm, system design/ implementation, interface study between RF/IF stage and digital signal processing part.

He is a member of IEEE, KICS and IEEK.